



Repositorio Institucional de la Universidad Autónoma de Madrid
<https://repositorio.uam.es>

Esta es la **versión de autor** del artículo publicado en:
This is an **author produced version** of a paper published in:

Organic and Biomolecular Chemistry 19.41 (2021): 9031-9042

DOI: <https://doi.org/10.1039/d1ob01439k>

Copyright: © 2021 The Royal Society of Chemistry

El acceso a la versión del editor puede requerir la suscripción del recurso
Access to the published version may require subscription

Water Biocatalytic Effect Attenuates Cytochrome P450-Mediated Carcinogenicity of Diethylnitrosamine: A Computational Insight

Emadeldin M. Kamel^{1,2}, Al Mokhtar Lamsabhi^{2,3,*}

¹Chemistry Department, Faculty of Science, Beni-Suef University, Beni-Suef 62514, Egypt.

²Departamento de Química, Módulo 13, Universidad Autónoma de Madrid, Campus de Excelencia UAM-CSIC Cantoblanco, 28049 Madrid, Spain. mokhtar.lamsabhi@uam.es

³ Institute for Advanced Research in Chemical Sciences (IAdChem), Universidad Autónoma de Madrid, 28049 Madrid, Spain.

ABSTRACT:

The mechanism-based mutagenicity and carcinogenicity of diethylnitrosamine (DEN) is believed to act through interaction with cytochrome P450 (P450) enzymes. DFT calculations to explore the conceivable mechanisms underlying the reaction of P450 with DEN with and without water as a biocatalyst were performed. The results shed light on the water biocatalytic role in lowering the H-abstraction energy barriers because of the electrostatic effect driven by hydrogen bonding. Our DFT analysis revealed how metabolites are formed in the dealkylation (toxification) and denitrosation (detoxification) pathways. Also, our findings uncovered the active position of DEN vulnerable to P450 interaction. Two factors are controlling toxification and detoxification rates; stability of denitrosation products and HS rebound barrier of α -pathway. Thus, water biocatalytic attenuation of DEN carcinogenicity was attained by stabilizing denitrosation products and slacken the α -HS rebound process. Docking and MD simulations were performed to assess the binding modes of DEN to P450's active site and to inspect the denitrosation and dealkylation processes, respectively.

KEYWORDS:

Cytochrome P450, density functional calculations, diethylnitrosamine, reaction mechanisms, metabolism, carcinogenicity.

INTRODUCTION

Cytochrome P450 (P450) heme-thiolate enzymes are noteworthy ubiquitous diverse oxidative catalysts that are found throughout nature.^{1, 2} Some P450s play a vital role in detoxication and, paradoxically, the formation of reactive metabolites of huge number of xenobiotics that have adverse influences on DNA, lipids and proteins.³⁻⁵

An accurate conception of the interaction mechanisms of P450s with xenobiotics by computational analysis would provide more trustworthy predictions of the drug-enzyme interaction mechanisms and reactivity than those already figured out.⁶ Since the great progress in DFT, which is the preferred method for studying bioinorganic systems like P450's active site, computational chemistry has increased the curiosity toward P450's problem to figure out the debates around the catalyzed C-H hydroxylation mechanism (also called Rebound mechanism).² The C-H hydroxylation, catalyzed by P450s, is one of the major metabolic processes by which toxic and endogenous materials are metabolized by our biosystems,⁷⁻¹¹ this mechanism is agreed to proceed via initial hydrogen abstraction, followed by rebound of the alkyl radical to the oxygen of the iron-hydroxy species.^{12, 13} This mechanism involves two-state reactivity (TSR) nascent from the two degenerate ground states of compound I (Cpd I) that was modeled by ferryl-oxene (Por^{+}FeO) species with HS^{-} as a proximal ligand, the TSR are low-spin (LS, doublet) and high-spin (HS, quartet).¹⁴⁻¹⁷ The TSR principal postulates a competition between two parallel reaction routes, and the predominant pathway is substrate and environment dependent.¹¹ A typical C-H hydroxylation reaction mechanism reveals a doubled profile as a result of the HS and LS states, these two profiles stay close in energy throughout the H-abstraction phase then bifurcate during the rebound step.² While The HS state mechanism shows a significant rebound transition state energy barrier, the LS pathway is basically proceeds via barrier-free mode.¹⁸ Intrinsically, the C-H hydroxylation reaction involves TSR, in which the HS route is stepwise with a limited radical intermediate life time, whereas the LS pathway is concerted with ultrashort radical intermediate life time.^{2, 18} On the contrary, the LS and HS pathways are concerted in case of C-H hydroxylation of N,N-dimethylaniline.^{19, 20}

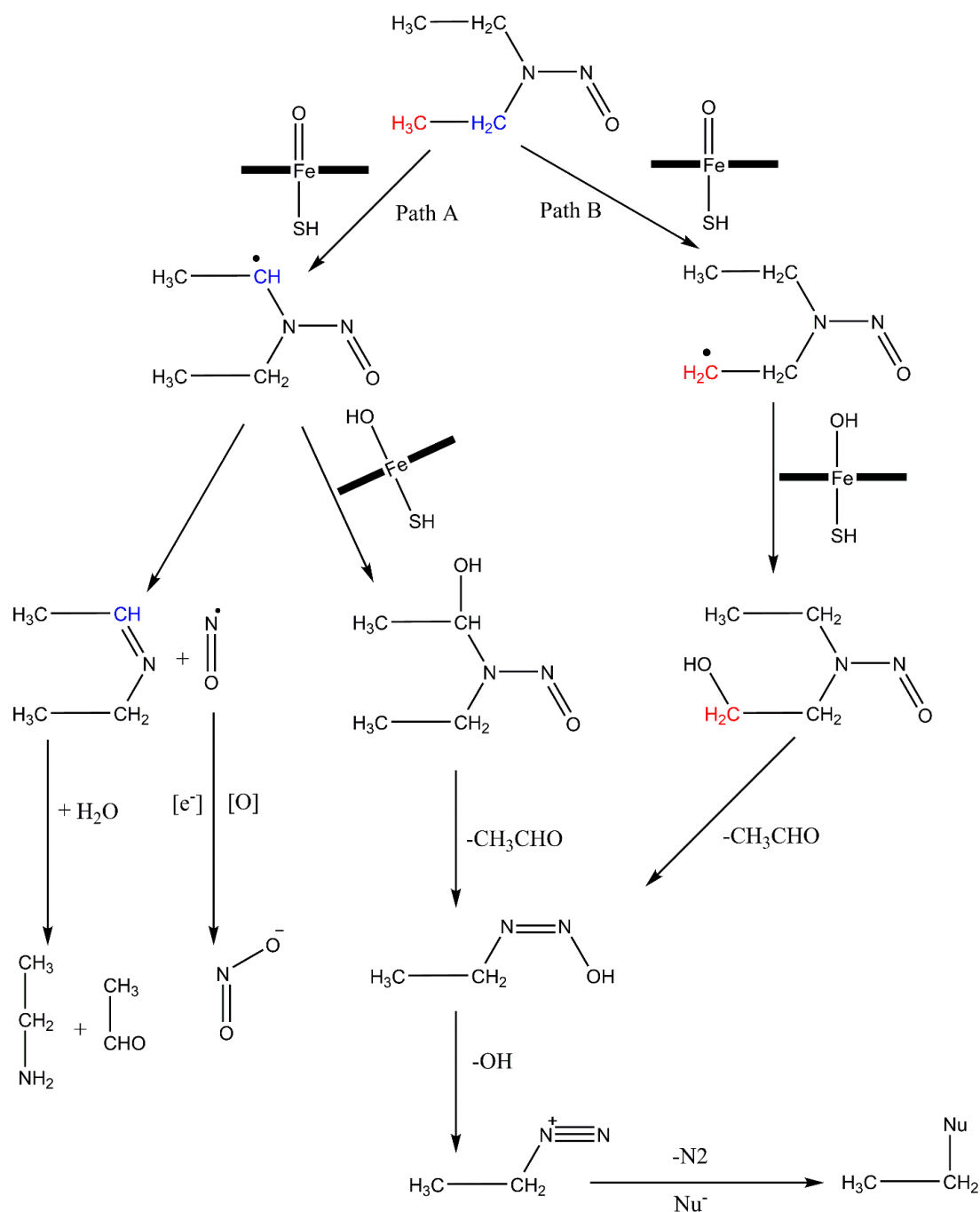
Water is a small ubiquitous molecule in biosystems that sometimes considerably perturbs the electronic nature of P450's active site and participates in the biochemical transformations.²¹ Essentially, water is playing a sizable role in the catalytic cycle of P450s where in the so-called "resting state" water act as a distal ligand, which is replaced upon substrate entry with another water molecule.^{22, 23} Differently, the pentacoordinate intermediate resulting from this replacement exhibits a redox potential such that it can be reduced, unlike the resting state, through the thereabout reductase enzyme.²³ Also, during the formation of Cpd I via protonation of its precursor (Cpd 0), a water molecule is produced close to the oxygen of the P450's active site.²⁴ The formed hydrogen bond between this water molecule and the oxo atom strengthens throughout the initial H-abstraction of P450s pathways merely due to the increment of the negative charge on the oxo atom.²³ Interestingly, a single water molecule was shown to lower the H-abstraction activation barrier of P450 reactions as a result of electrostatic interaction with the oxo atom of Cpd I.^{23, 25}

The main objective of the present work is to figure out the α - and β -hydroxylation mechanisms of Diethylnitrosamine (DEN) by DFT analysis, as well as the denitrosation pathway. Meanwhile the biocatalytic influence of one and two water molecules on the three competing mechanisms will be also presented in the exploration. Cpd I is used to model P450's active site to detect which route is kinetically more favored with and without water as a biocatalyst. Docking and Molecular Dynamics (MD) simulations techniques will be employed to assess DEN-P450 complex's binding interactions and to follow the course of denitrosation and dealkylation processes, respectively.

RESULTS AND DISCUSSIONS

Diethylnitrosamine (DEN), also known as *N*-nitrosodiethylamine, is one of the most common chemical carcinogens activated by mammalian P450s with the ability to initiate and promote tumors in different organs of the human body.²⁶ Generally, bioactivation of DEN generates preneoplastic lesions and subsequently hepatocellular carcinoma.²⁷ DEN metabolic mechanism of activation (toxification) mediated by P450 is believed to proceed

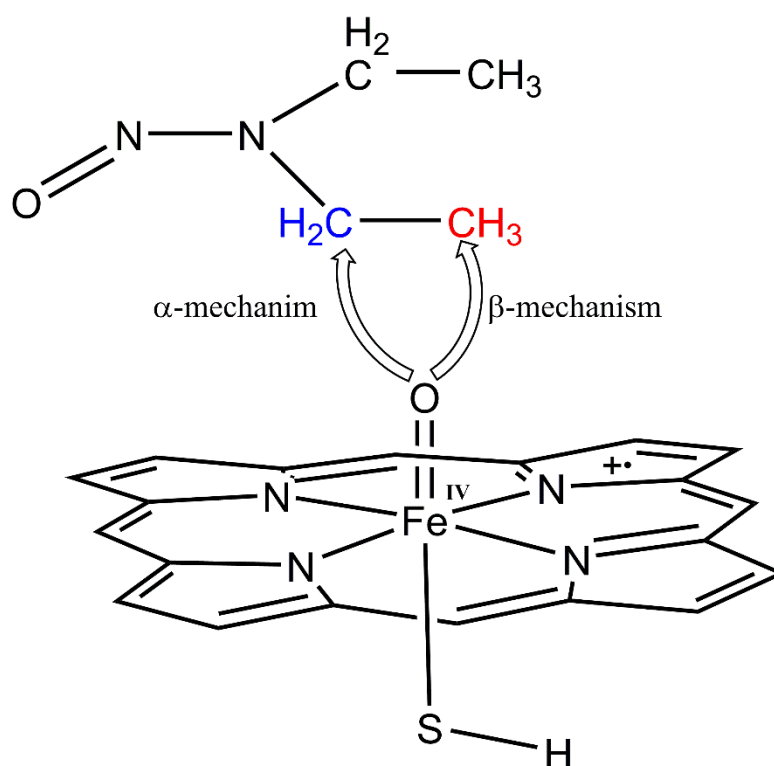
via α -hydroxylation process, this α -hydroxylation process is generally agreed to involve an initial H-abstraction from DEN to P450's iron-oxo species instead of the alternate single electron oxidation implicated for some amines.^{2, 28, 29} Following the H-abstraction step, recombination of the nascent α -nitrosamino radical with the hydroxyl radical produced from P450's Fe-OH.²⁸ The resulting α -hydroxynitrosamine rearranges to afford an aldehyde and an alkyl diazohydroxide, the latter alkylate DNA probably via an alkyl nitrenium ion or carbocation resulting in tumor initiation.^{27, 30} In addition to the toxification reaction, a denitrosation reaction (detoxification) may also occur to yield nitrite. Nitrite formation is an alternative route for the carcinogen toxification (dealkylation) pathway.³¹⁻³³ In the denitrosation mechanism, the H-abstraction step-resulted α -nitrosamino radical is fragmentized into nitric oxide and imine, which is hydrolyzed to acetaldehyde and ethylamine.³³ Jointly, the dealkylation and denitrosation pathways of DEN could occur, and also some investigation demonstrated that both are catalyzed by the same P450.^{16, 33} The α - and β -dealkylation mechanisms along with the denitrosation mechanism of DEN are represented in Scheme 1.



Scheme 1. Proposed mechanisms for DEN-P450 catalyzed biotransformation; Path A: initial α -H abstraction as a key step affording α -nitrosamine radical intermediate for the subsequent dealkylation and denitrosation pathways; Path B: β -H abstraction as a precursor for β -dealkylation route.

The conceivable pathways for the reaction of DEN with P450 Cpd I using DFT were assessed by setting up a model as shown in Scheme 2. Two possible mechanisms for the reaction of DEN with P450 were predicted, which differ mainly in how the oxo-ferryl

species interacts with DEN (Path A and Path B, Scheme 1). Path A is initiated by α -hydrogen abstraction from DEN, while Path B is started by β -hydrogen abstraction. The biocatalytic influence of one and two water molecules on the two pathways of DEN-P450 reaction was examined. Figures 1, 2 and 3 represent the obtained energy profiles (in kcal mol⁻¹) and key geometric features at the UB3LYP/B2//B1+ZPE(B1) and UB3LYP (SCRF)/B2//B1+ZPE(B1) levels for both the HS and LS states of the DEN-P450 reaction, DEN-P450 reaction catalyzed by one water molecule and DEN-P450 reaction catalyzed by two water molecules, respectively.



Scheme 2. Model for our DFT analysis for the possible pathways for DEN-P450 interactions.

Path A: Initially, the Reactant complex (RC_α) in the HS and LS states is stabilized by weak hydrogen-bonding interaction between one α -hydrogen of DEN and the oxo species giving rise to degenerated LS and HS (about 0.1 kcal mol⁻¹ as a gap between both states). This gap is slightly perturbed when one and two water molecules are involved in the interaction, the energy of the doublet with respect to the quartet state is about 0.2 kcal mol⁻¹ in both cases. In the water-free system the O \cdots H distance is ~ 2.4 Å. In the presence of additional water

molecules, the water is normally hydrogen bonded to the oxo moiety in way such that it does not interfere with the substrate with O...H distance between DEN and Fe^{IV}=O ~ 2.9 and 2.8 Å for one and two water molecules, respectively. The weaker hydrogen bonding between DEN and P450 in case of water presence is mainly due to the distribution of electrons in forming stronger hydrogen bonds with water (O...H distance ~ 1.9 Å for one water and ~ 1.8 and 1.9 Å for the two water molecules).

Following up the rate determining step for both the LS and HS pathways, which is the α -H atom transfer from DEN to the oxo-ferryl moiety of Cpd I, the LS transition state (²TS-H _{α}) showed a higher energy barrier than its HS parallel (⁴TS-H _{α}) in the water-free system (14.9 vs 14.1 kcal mol⁻¹), this dissimilarity could be observed from the arrangement O...H...C distances (~ 1.3 and 1.2 Å for LS vs 1.2 and 1.3 Å for HS, respectively). Furthermore, the two transition states (^{2,4}TS-H _{α}) exhibit the geometry of H-abstraction transition states with an almost collinear arrangement of the O...H...C species^{14-16, 34} (O...H...C angles of 165-167°). Contrastingly, the H-abstraction energy barriers calculated with water are generally lower than its water-free counterpart, this barrier lowering is of electrostatic origin in all cases.²³ The UB3LYP (SCRF)/B2//B1+ZPE(B1) energy barrier lowering is 3.0 kcal mol⁻¹ for LS and 1.0 kcal mol⁻¹ for HS state in one water-catalyzed system, whereas in two water system the LS and HS H-abstraction barrier is reduced by 0.96 and 1.44 kcal mol⁻¹, respectively. It should be noted that, the H-abstraction barrier for the LS state is higher than its HS counterpart only with one water molecule system²³ indicating the discrimination of LS and HS H-abstraction energy barriers of DEN-P450 reaction with and without water as a result of the close energy values. This output confirms that the reaction is ruled by TSR as previously reported for the C-H hydroxylation of alkanes.^{14, 15} Comparing geometries of ^{2,4}TS-H _{α} for systems with and without water, the shape is generally retained with bond angles ranging between 165-166° for one water system and 167-170° for two water system. For the O...H...C moiety, the bond distance of O...H is shortened by 0.05 Å for LS and lengthened by 0.03 Å for HS in case of one water system, whilst in two water system it is increased by 0.04 and 0.05 Å for LS and HS

state, respectively, this is probably due to the oxo species electron deficiency as a result of the electrostatic effect of forming two hydrogen bonds with two water molecules (bond distances ~ 1.8 and 2 Å). The obtained C \cdots H distance with one water is typically longer by 0.05 Å for LS and shorter by 0.02 Å in case of HS state, while the LS and HS distances are lowered by 0.006 and 0.04 Å, respectively, because of the O \cdots H stretching. Other geometrical features of the H-abstraction transition states are also included in all cases, involving decreasing in Fe-S bond length, increasing of Fe-O bond length, minor breathing of the porphyrin, partial return of the Fe into the porphyrin plane and the increased imaginary frequency¹⁴.

Subsequent to the H-transfer from DEN to the oxo moiety of Cpd I, a radical intermediate is formed, $^{2,4}\text{INT}_\alpha$, which is a complex of $\alpha\text{-DEN}^\bullet$ and FeOH(PorSH) with $\alpha\text{-CH}^\bullet$ of the substrate is still coordinated to the hydroxyl group of the Fe-OH complex³⁴. Here the situation is similar in that the LS is laying below the HS state in all cases with energy difference less than 0.3 kcal mol⁻¹ but differs in the obviousness of the water biocatalytic effect on the stability of intermediates in a way such that water involvement provides more stable radical intermediates by ~ 3 kcal mol⁻¹. As expected, the O \cdots C distance in the water-free system (~ 3.6 Å for LS and 3.5 Å for HS) is shorter than its water system counterpart (~ 4.8 Å for one water and ~ 4.9 Å for two waters), this could probably explain the intermediate energy depression of the water interacted system than the free one. It should be noted that, the N-N bond length of DEN radical is larger than that of the preceding $^{2,4}\text{TS-H}_\alpha$ and $^{2,4}\text{RC}_\alpha$ by ~ 0.069 Å in the water-free system, while in the one-water system it is larger by ~ 0.075 Å. Interestingly, the variation of the N-N distance with two water molecules from $^{2,4}\text{RC}_\alpha$ to $^{2,4}\text{INT}_\alpha$ provides a preliminary picture to the effect of water in enhancing the denitrosation of DEN by lengthening the N-N distance of $^{2,4}\text{INT}_\alpha$ by 0.105 Å over that of $^{2,4}\text{RC}_\alpha$ and 0.076 Å for $^{2,4}\text{TS-H}_\alpha$. In addition, we can conclude that detoxification process of DEN becomes more willing after the $\alpha\text{-H}$ -abstraction from DEN and with presence of water as biocatalyst.

After radical intermediates cluster formation, $^{2,4}\text{INT}_\alpha$, two conceivable routes are proposed for these intermediates to complete its P450-catalyzed biotransformation, a major one (dealkylation or toxification pathway) involving the rebound of these intermediates to OH to afford α -hydroxydiethylnitrosamine ($^{2,4}\text{P-OH}_\alpha$) and Fe(PorSH) and a minor one (denitrosation or detoxification pathway) proceeds via cleavage of N-N bond to produce imine, nitric oxide and FeOH(PorSH) ($^{2,4}\text{P-NO}$). For all mechanism, the relative enthalpies of N-N bond cleavage transition state are neglected as a result of being lower than its preceding intermediates, in addition to the proceeding of the LS rebound step via a concerted mechanism, whereas the HS route is a two-step process with a significant rebound energy barrier as previously reported for alkane hydroxylation^{14, 16}.

How water biocatalytic effect influences carcinogenicity of DEN?

Based on the experimental results depicting the metabolism of DEN in human liver, the formation rates of deethylation and denitrosation products were measured at different DEN concentrations^{8, 35}. The previous reports indicated that, denitrosation followed a similar pattern to that of the dealkylation, and the denitrosation was estimated to explain around 17-24% of P450-DEN catalyzed biotransformation according to the calculated rates of NO_2^- and acetaldehyde formations³⁵. The denitrosation rate of DEN was found to be higher than that of *N*-nitrosodimethylamine (NDMA)³⁵, which likely explains the increased stability of DEN denitrosation products (water-free) (12.2 and 12.5 kcal mol⁻¹ for LS and HS, respectively) when compared to that of NDMA at the same level of theory (5.0 and 5.1 kcal mol⁻¹ for LS and HS, respectively)¹⁶. However, both DEN and NDMA activation mechanisms are very similar in possessing TSR characteristics, LS free rebound barrier route and negligible N-N bond cleavage transition states¹⁶. These outcomes would bring to mind that, stability of the denitrosation products, $^{2,4}\text{P-NO}$, is one of the main factors controlling the denitrosation percentage of P450-mediated *N*-Nitrosodialkylamines biotransformation. This inference is confirmed by the fact that, the denitrosation of NDMA accounts for about 14-20% of the catalyzed biotransformation³⁶, although both compounds follow the same biotransformation pathway. Consequently, one of the reasons we could

think about regarding this large variation in DEN and NDMA detoxification portion is the stability of the detoxification products. Thus, stabilizing the denitrosation products would promote the detoxification pathway of *N*-Nitrosodialkylamines and consequently attenuates its carcinogenicity.

To be more realistic, two possible conformers for the denitrosation products in case of water-catalyzed systems were studied. In the one water mechanism (Figure 2), the first conformer involves strong electrostatic hydrogen bonding (distance ~ 1.7 and 1.8 Å for LS and HS, respectively) between the water molecule and the oxygen atom of the ferryl hydroxy species ($^{2,4}\text{P-NO}_1$) in which the water molecule is not facing the released imine and nitric oxide, whereas the second one ($^{2,4}\text{P-NO}_2$) includes a water molecule facing the imine and nitric oxide. At this position, water molecule forms three hydrogen bonds with nitrogen of the imine (~ 1.8 Å), N atom of nitric oxide (distance ~ 2.7 and 2.4 Å for LS and HS, respectively) and Hydrogen of the Fe-OH moiety (~ 1.7 Å). In case of two water system (Figure 3) the situation is not so different, where a conformer is formed via two water molecules are hydrogen bonded to the oxo atom of the ferryl hydroxy species (one molecule distance ~ 1.8 Å for LS and 2.1 Å for HS vs 1.7 Å LS and 1.9 Å HS distance for the other molecule), while the other conformer includes one water molecule bonded to the oxo of Fe-OH (~ 1.9 Å) and another molecule bonded to N of the imine (~ 1.8 Å), N atom of NO (distance ~ 2.7 Å) and Hydrogen of the Fe-OH moiety (~ 1.7 Å). Normally, the high extent of hydrogen bonding provides a more stable structure, and consequently the second conformer in both cases (one and two water systems) possessing lower energy than the first conformer. In addition, the significantly high N-N distance in the second conformer provides a clear thought to doubt in being the one of interest.

Coming back to the effect of water on the denitrosation routes of P450-DEN reaction, the LS and HS energies of the optimized denitrosation products ($^{2,4}\text{P-NO}_{1,2}$) gradually decrease as the number of water molecules increases. Where in the water-free system the $^{2,4}\text{P-NO}$ energies are -12.2 and -12.5 kcal mol $^{-1}$ for doublet and quartet states, respectively. In the

one water system, the detoxification product is laying below that of the water-free system in both conceivable conformers with LS and HS energies -13.7 and -13.8 kcal mol⁻¹, respectively for the first conformer, whereas the second conformer energies are -14.6 and -16.0 kcal mol⁻¹ for doublet and quartet states, respectively. On the other side, The LS and HS energies of ^{2,4}P-NO₁ in case of two water molecules catalyzed pathways are -16.9 and -19.5 kcal mol⁻¹, respectively, whilst ^{2,4}P-NO₂ possessing energies of -19.6 and -22.9 kcal mol⁻¹ for LS and HS state, respectively. Obviously, there is a gradual increment in the stability of detoxification products with water extent. Although we are dealing with two different P-NO conformers in water systems, both (^{2,4}P-NO_{1,2}) conformers are still showing much lower energies than corresponding denitrosation products (^{2,4}P-NO) in the water-free system. This is an indication to our deduction stating that, water biocatalytic effect stabilizes denitrosation products of P450-DEN catalyzed biotransformation and consequently stability of these products is one of the factors controlling detoxification rate as previously illustrated. Thus, we can conclude that water has a crucial effect in diminishing carcinogenicity of DEN through promoting detoxification route.

Besides stabilities of denitrosation products, a second major factor contributing significantly to the enhancement of detoxification routes of DEN biotransformation is the energy of the HS rebound barrier (⁴TS-reb_α) of α-pathway. The low denitrosation portion (17-24%)³⁶ of p450-DEN catalyzed biotransformation accounts for a strong priority of the radical intermediates (^{2,4}INT_α) to be hydroxylated (^{2,4}P-OH_α) rather than fragmentize to denitrosation products (^{2,4}P-NO), which is in a good agreement with our calculations, whereas the energy difference between toxification and detoxification products in the water-free system is about 40 kcal mol⁻¹. In the one water-catalyzed system, the energy differences are decreased to be about 38 and 36 kcal mol⁻¹ for the first and second conformer, respectively, while these differences are decreased dramatically in case of two water system to reach ~ 32 kcal mol⁻¹ for the first conformer and ~ 29 kcal mol⁻¹ for the second one. Recalling the fact that the LS rebound process is barrier-free in all cases, it is likely that this route contributes significantly to the hydroxylation pathway. Alternatively,

the HS rebound step involves a significant barrier that possibly contributes to denitrosation process as a less favorable side reaction.¹⁶ Consequently, a considerable HS rebound barrier will allow adequate lifetime for the radical intermediates to feed both the α -hydroxylation and denitrosation in the HS route.¹⁶ This is suggestive for, the HS rebound barrier is one of the factors affecting the toxification and detoxification of DEN biotransformation. In general, there is a gradual increase in the HS rebound barrier as we moved from free to two water system. In the free system, the HS rebound barrier energy is quite meager (2.6 kcal mol⁻¹), whereas in one and two water systems this barrier rises to 3.1 and 7.6 kcal mol⁻¹, respectively. This information is of particular interest since it reveals that, the significant elevation in the HS rebound barriers with water extent will provide more lifetime for α -nitrosamino radicals to consolidate the detoxification pathways and consequently assist in detoxifying DEN in its P450-catalyzed biotransformation.

Although denitrosation products in all cases have close energies, but they differ considerably in both N-N and Fe-O...C distances. The N-N and Fe-O...C distances of quartet states is much larger than those of doublet states. In the water-free system, N-N distances were estimated to be 2.2 Å for LS and 2.5 Å for HS. While in the first conformer of the one water system, the N-N distances were \sim 1.9 Å for doublet and \sim 2.5 Å for quartet state. With respect to the first conformer of the two-water system, a 1.8 and 2.6 Å N-N distances were obtained for LS and HS states, respectively. One should notice the gradual decline in the LS N-N distance as we go from free to two water system. Regarding the N-N distances in case of water systems second conformer, were found to be unexpectedly larger than that of its first conformer rival (4.30 Å vs 4.33 Å for one water and 4.342 Å vs 4.343 Å for two water system). Besides the higher stability of the second conformer, the larger N-N distance would lead to more thoughts of considering these conformers are probably the prevailing ones. Form all these findings we could deduce that, the fragmentation of DEN in the denitrosation route is much more nominated for the HS product than its LS counterpart, nevertheless both products, ^{2,4}P-NO, in all mechanisms are finally turned into NO₂ and carbonyl (Scheme 1). Alternatively, the α -hydroxylation of

DEN is much more pronounced for the LS pathway as a result of being rebound barrier-free. Therefore, we can conclude that, the detoxification products of DEN are basically produced from the HS route with its significant rebound barrier, while the deethylation products are arisen essentially from the LS pathway with its free rebound barrier.

Path B: The relative energies of the optimized structures along path B were obtained relative to the doublet reactant complex of path A ($^2\text{RC}_\alpha$) by holding the view of both α - and β - positions are possibly having equal probabilities for the interaction with the ferryl oxo species of P450. Initially, one β -hydrogen atom of DEN is normally hydrogen bonded to the oxo moiety of Cpd I, yielding a slightly higher energy for HS states over those of LS states in all competing β -mechanisms. Unexpectedly, Path B reactant complexes in all cases, $^2,4\text{RC}_\beta$, have higher energies than those of its contestant Path A counterparts ($^2,4\text{RC}_\alpha$) by energies 2-3 kcal mol⁻¹ at the same level of theory.

As expected, the β -hydrogen atom transfer steps in all systems (without and with water), $^2,4\text{TS-H}_\beta$, showed energy barriers higher than those of α -hydrogen abstraction. Where the energy difference is 5.3 and 3.6 kcal mol⁻¹ in the water-free system for HS and LS states, respectively and in the one water mechanism the differences are 5.8 kcal mol⁻¹ for LS and 5.5 kcal mol⁻¹ for HS states in favor of β -mechanism. Similarly, the LS and HS H-abstraction transition states in case of two waters β -mechanism are possessing higher energies over those of α -mechanism by 2.9 and 5.4 kcal mol⁻¹, respectively. The elevated energies of β -hydrogen abstraction transition states are attributed to the thermodynamically more favorable secondary radicals in α -mechanism over the primary ones in β -mechanism as previously reported for C1 and C2-H hydroxylation of propane³⁷. In addition to, the arrangement O...H...C distances of α -mechanisms reveals a different pattern from those of β -mechanisms transition states in such that the former possessing longer H...C and shorter O...H distances than those of the latter, nevertheless the linearity of O...H...C arrangement is still conserved. Contrary to α -mechanisms, water has no remarkable effect on energies of H-abstraction processes. All these consequences would lead to the proposal

that, α -Hydrogen abstractions of P450-DEN catalyzed biotransformation is kinetically less favorable than those of the competing β -mechanisms.

Since charged systems are stabilized when the charge is dispersed or delocalized, the H-abstraction subsequently formed primary β -radical intermediates ($^{2,4}\text{INT}_\beta$) is thermodynamically less stable than the secondary α -radical intermediates by $\sim 19 \text{ kcal mol}^{-1}$ in case of water-free system. Whereas in the one water system, β -intermediates are higher in energy than α -intermediates by $22.4 \text{ kcal mol}^{-1}$ for LS state and $18.1 \text{ kcal mol}^{-1}$ for HS state. Similarly, the difference is nearly $16.5 \text{ kcal mol}^{-1}$ in case of two water system. The higher energies of α -intermediates over those of β -intermediates could be reflected from the lengthening of $\text{O}\cdots\text{C}$ distances of the latter. Also, we could note that water has no significant influence on stabilities of α -intermediates when compared with its effect on β -intermediates. In addition to, N-N distances showed nearly no variation along Path B contrary to Path A indicating no tendency for denitrosation during β -interaction. A tinny β -rebound barriers were obtained in all cases for both LS and HS states with subsequent formation of β -hydroxynitrosamine, which in most cases is of energy higher than α -hydroxynitrosamine especially for the HS state.

Our Path A and Path B comparative study indicated that Path A is much more predominant than Path B because of the reactivity of Path A reactant complex against those of Path B, the higher H-abstraction barrier of Path B and the thermodynamically less favorable primary β -radical intermediates. However, the H-abstraction from DEN is catalyzed by P450, but the reactivity of the process is depending on C-H bond strength. The bond dissociation enthalpies (BDE) of α - and β -C-H of DEN were calculated at the same level of theory. The results showed a correlation between H-abstraction energy and BDE, where BDE of α - and β -C-H were estimated to be 84.7 and $98.9 \text{ kcal mol}^{-1}$, respectively.

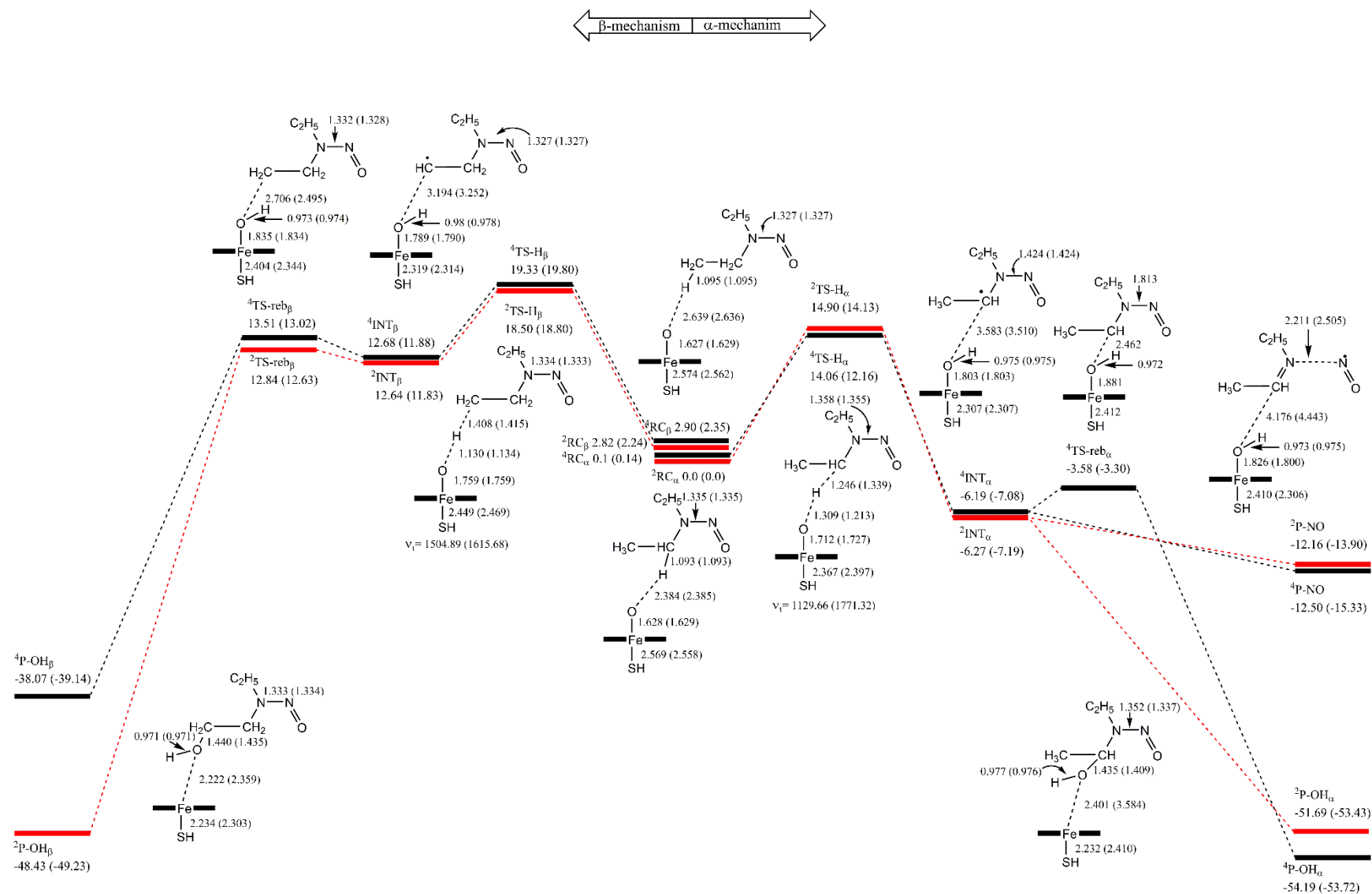


Figure 1. Energy profiles (in kcal mol⁻¹) for Paths A and B in case of water-free system as estimated at the B3LYP/B2//B1+ZPE(B1) (in parentheses) and the B3LYP (SCRF)/B2//B1+ZPE(B1) levels, along with geometrical features for the reaction species in both LS and HS (in parentheses) states.

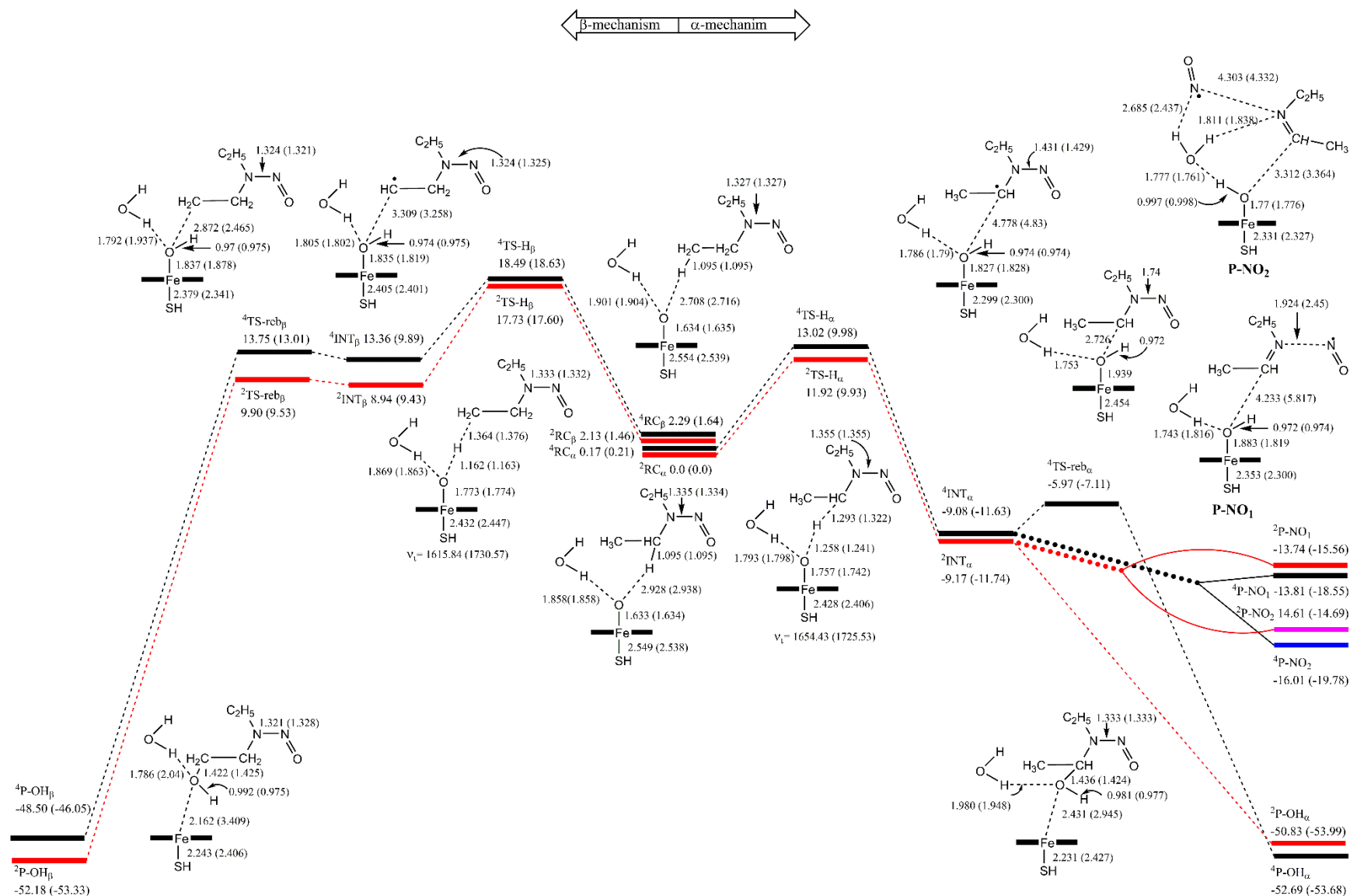


Figure 2. Energy profiles (in kcal mol⁻¹) for Paths A and B in case of one water system as estimated at the B3LYP/B2//B1+ZPE(B1) (in parentheses) and the B3LYP (SCRF)/B2//B1+ZPE(B1) levels, along with geometrical features for the reaction species in both LS and HS (in parentheses) states.

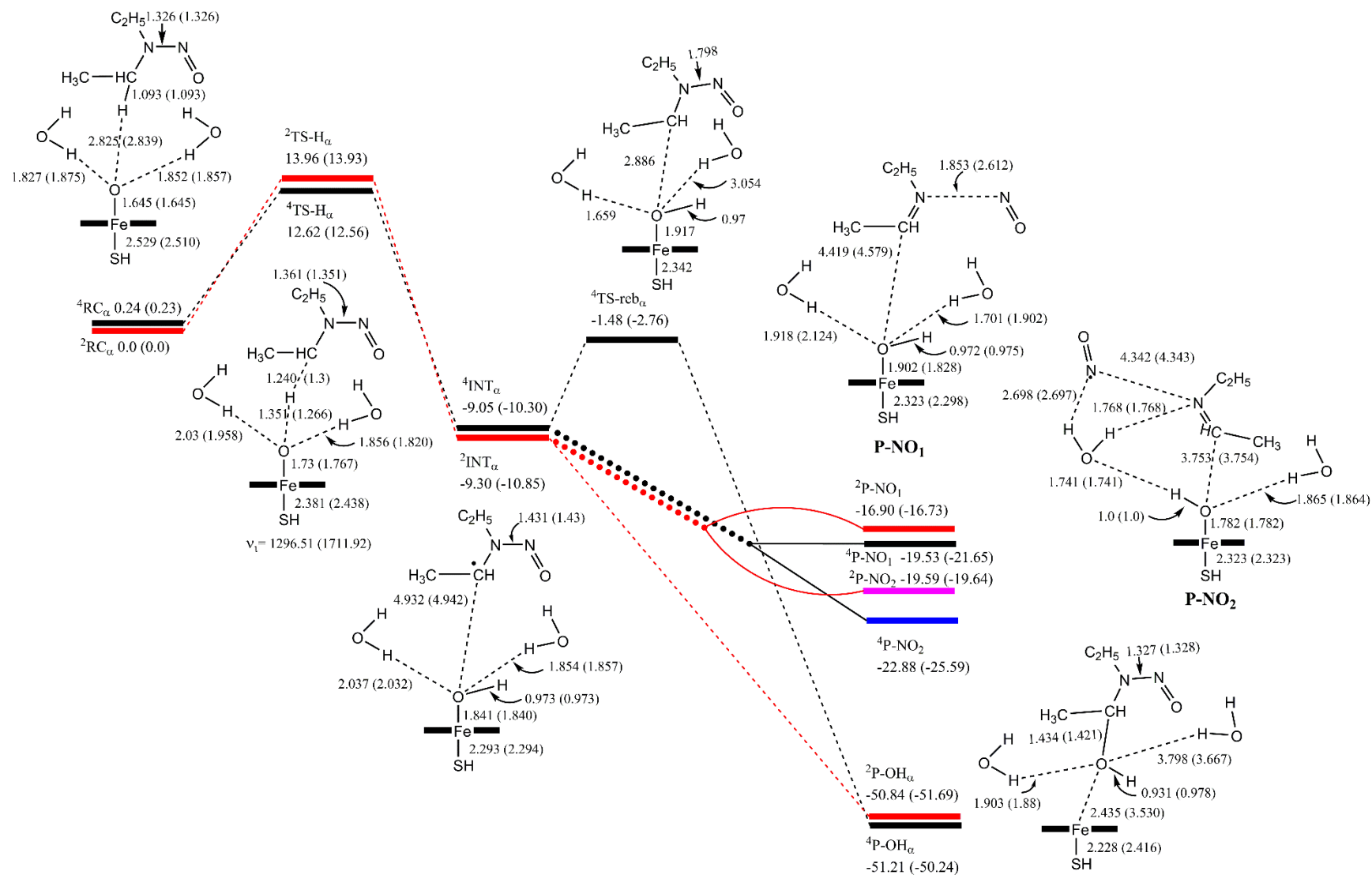


Figure 3. Energy profiles (in kcal mol⁻¹) for Path A as estimated for two water system at the B3LYP/B2//B1+ZPE(B1) (in parentheses) and the B3LYP (SCRF)/B2//B1+ZPE(B1) levels, along with geometrical features for the reaction species in both LS and HS (in parentheses) states.

The ab initio MD simulations using the atom-centered density matrix propagation (ADMP) method was performed to go through the denitrosation and dealkylation processes. Focusing on the last step of the α -pathway, a total of 100 trajectories of each spin state were sampled by ADMP simulation to follow the evolution of the transition state TS-reb $_{\alpha}$ in HS and LS states, as represented in Figure 4. It is worth to note that, due the finite number of trajectories and the convergence struggling of some calculations we cannot claim that our results are statistically accurate. Our statement is, however, an intent to highlight the trends to get P_{OH} and P_{NO} products in its higher and lower spin states. In fact, among the pathways examined, nitro departure is the most dominant product in both spin states. As depicted in Figure 4, more than 95 % of trajectories pointed out that the dominant pathway collapsed to a denitrosation product when HS is considered, whereas this percentage descend to 65 % in the LS.

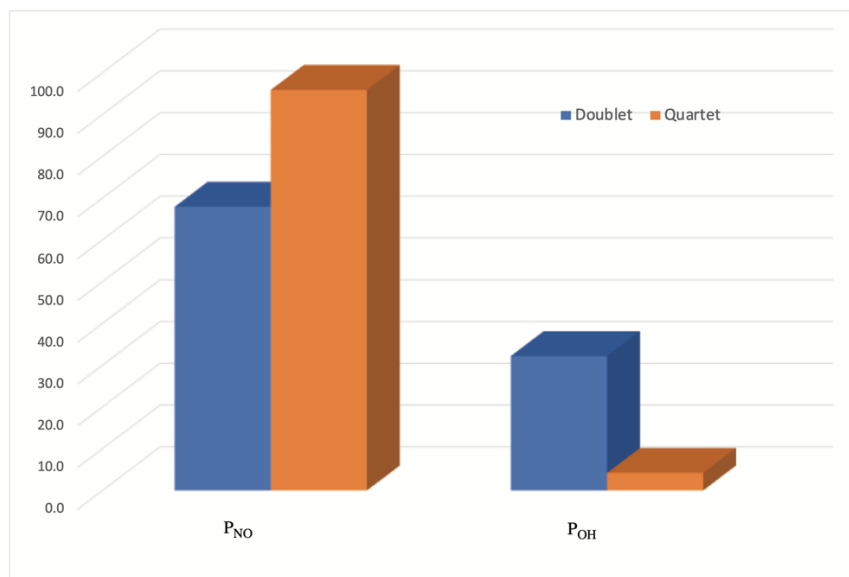


Figure 4. Percentage of trajectories leading to P_{OH} and P_{NO} products at HS and LS states among 100 of simulated AMDP trajectories in each case.

Although the percentage to lead the denitrosation product is higher, a careful analysis of the potential energy variation along the ADMP simulation shows an energy increase to allow the nitro group departure. In Figure 5 we present the relative potential energy along the ADMP simulation for four examples of trajectories obtained from the transition state TSreb- α of 200 fs. These graphs also contain the changes of the bond lengths for the most

important bonds: **(a)** and **(b)** represent the processes at LS state while **(c)** and **(d)** reflect the variations at HS state. The most important information that can be collected from this figure is the energy demanding to get P_{NO} product in both spin states. During the dynamic simulations, to gain P_{NO} product at HS and LS, the relative potential energy remains positive even if the bonds rupture is apparent. As shown in Figure 5 (b) and (d), the separation of the fragments began at ~ 20 fs is reflected by an increase of the distance between the nitrogen atoms in the denitrosation and the lengthening of HO—C bond. This detachment is more rapid in the HS which reaches a separation at ~ 3.7 Å between the nitrogen atoms at 200 fs while in LS this distance attains ~ 2.1 Å at the same time of the process. The relative potential energy in the later is ~ 12 kcal/mol while for the lower spin state process is ~ 26 kcal/mol. In contrast, the dealkylation represented by the departure of OH within Cpd I is easy-going and faster than denitrosation (Figure 5 (a) and (c)). So, at ~ 40 fs in the HS pathway the relative potential energy becomes negative, and the formation of C—OH bond stands to a covalent character reaching ~ 1.3 Å at 75 fs. In the LS process the progression is slower, and the covalency of C—OH bond is attained at ~ 120 fs.

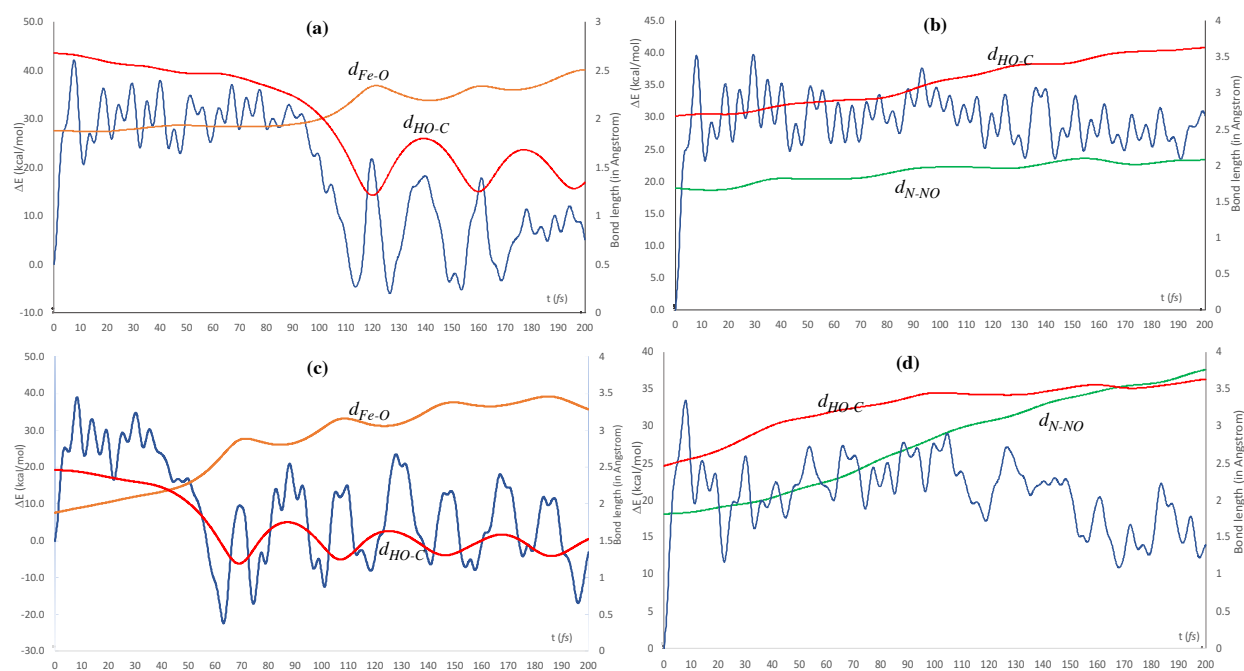


Figure 5. The relative potential energy (in kcal/mol) during the ADMP simulation of 200 fs from TS-reb_α in HS and LS to get the products: (a) ²P_{OH}, (b) ²P_{NO}, (c) ⁴P_{OH} and (d) ⁴P_{NO}. the variation of the most important breaking and forming bonds during the simulation for each case is also reported.

To figure out the compatibility of DEN to the binding pocket of P450, a molecular docking analysis was performed using AutoDock Vina. Three isozymes were employed for this study, namely CYP3A4, CYP2D6 and CYP101D2. The First two were selected because these P450 isoform is believed to be involved in the biotransformation of large number of xenobiotics^{12, 38, 39}, whereas CYP101D2 isoform was employed because its binding site displays Cpd I form (oxo ferryl porphyrin species) of P450.

The most abundant CYP enzyme in both the liver and the small intestine, CYP3A4, is of particular relevance because it is known to catalyze the metabolism of about 50% of medicinal drugs.^{40, 41} After visual inspection of the docking pose of DEN-CYP3A4 complex (Figure 6), DEN was shown to occupy the main active site cavity of the enzyme with a binding energy of (-6.8 kcal/mol). Interestingly, a polar bond was detected with the heme group existing in the main binding pocket of the enzyme reflecting the activity of DEN against this P450 isoform. In addition, hydrophobic interactions were obtained with four known significant key residues namely, Thr309, Ile369, Ala370 and Leu482.³⁹ These outcomes suggest the activity of DEN against this P450 isozyme.

The stability of DEN-P450 complex (CYP2D6 isozyme, PDB ID: 2F9Q) was estimated from the relatively low binding affinity (-7.2 kcal/mol) obtained by molecular docking assessment, as represented in Figure 7. Besides, DEN was shown to dock into the central cavity of the main binding pocket with the heme group surrounded by the hydrophobic residues Phe120, Ala305, Thr309, Val370 and Met374. The residues Phe120 and Ala305 was shown to be important key residues involved the catalyzed biotransformation of this P450 isozyme.³⁸ This information is of particular interest since it shed the light on the compatibility of DEN to P450's binding site. The existence of the favorable π - π interactions among aromatic moieties plays substantial role in recognizing molecular orientation and in adjusting drug conformation to fit the target's active site. Therefore, the

availability of one phenylalanine residue (Phe120) in the binding site of this complex offers a high probability for the electrostatically favorable π - π interaction. This inference is confirmed by the fact that DEN interacts with phenylalanine residues by the favorable interaction edge-to-face and offset stacked orientation types instead of the unpreferred face-to-face and edge-to-edge orientations ⁴².

The optimal docking pose for DEN-P450 interaction (CYP101D2 isozyme, PDB ID: 3NV5) was chosen after several attempts based on its conformation and binding energy (Figure 8). A lower binding energy was obtained for this complex (-7.4 kcal/mol) indicating the stability of the complex formed. Docking outputs showed that DEN is located in the internal cavity of the enzyme linked to oxo ferryl porphyrin moiety and encased by the hydrophobic residues Val117, Ala297, Thr301, Leu362 and Leu366. Obviously, the best docking pose is that with the ligand exhibits polar interaction with the oxygen of the oxo ferryl porphyrin unit as shown in Figure 7. This information agrees with the proposed mechanisms for our DFT calculations for DEN-P450 interactions. Contrary to the other isozyme, the availability of polar and hydrophobic interactions in this docking output confirms Cpd I as the proper active site form of P450 and confirms the suitability of this isozyme for this study so as to be in coincidence with DFT calculations. The surface representation of P450 with DEN binds to the active site main cavity is shown in Figures 6 and 7. In general, the result of our molecular docking investigation suggests the activity of DEN against the active site of P450 through polar bonds, hydrophobic interactions and π - π interaction.

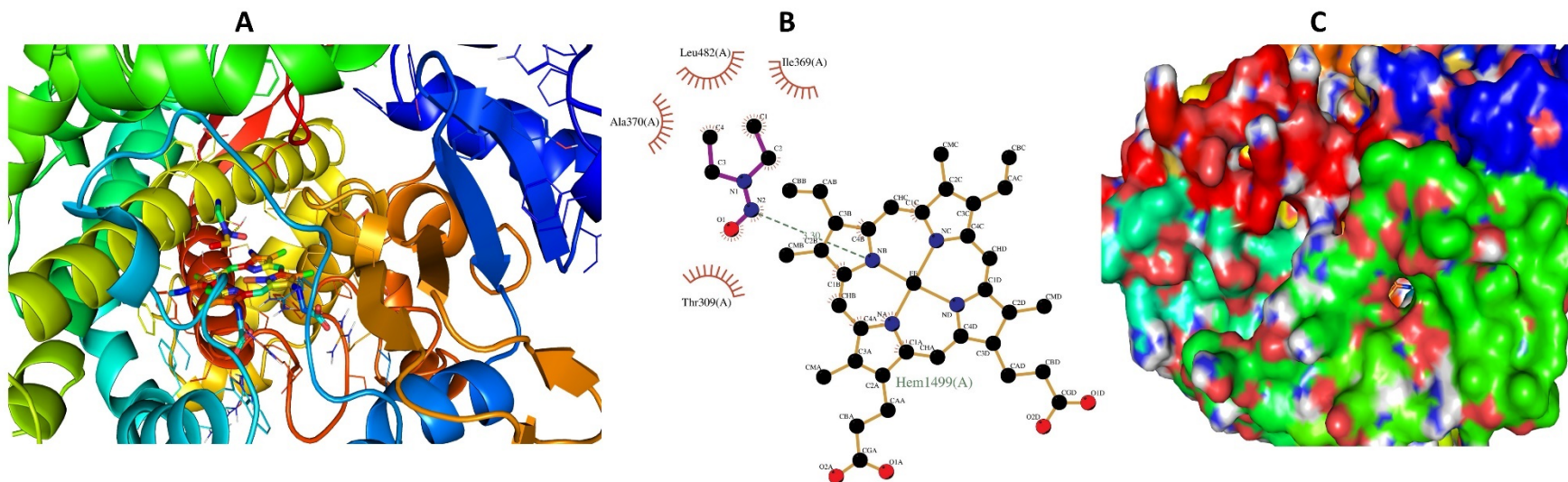


Figure 6. Binding site of DEN with P450 (CYP3A4 isozyme), DEN and P450's binding pocket are represented as tube model, while residues are shown as stick model (A), surface representation of the active site of P450 occupied by DEN (C), residues exhibiting polar and hydrophobic interactions with DEN are presented in the middle (B).

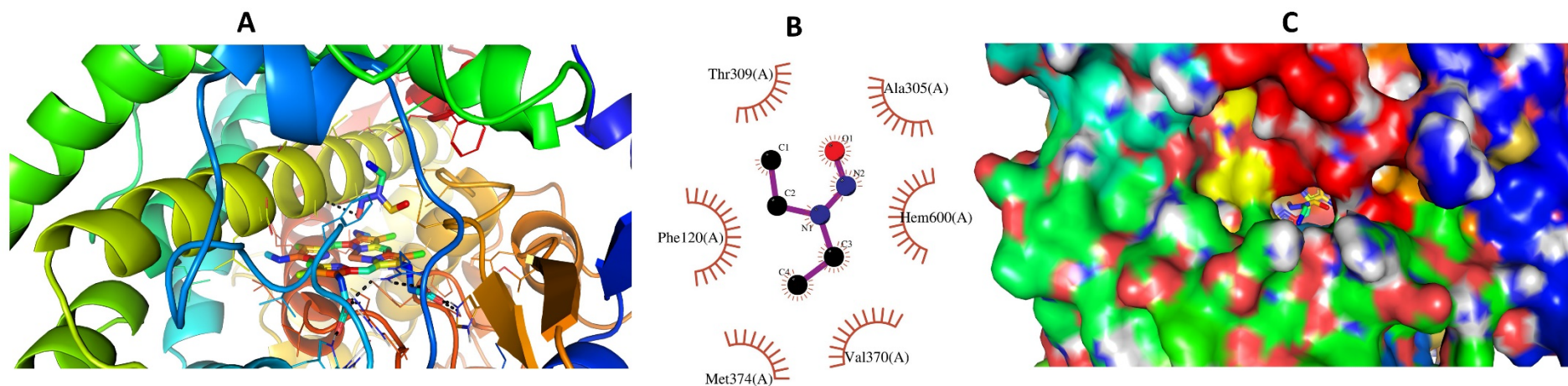


Figure 7. Binding site of DEN with P450 (CYP2D6 isozyme), DEN and P450's binding pocket are represented as tube model, while residues are shown as stick model (A), surface representation of the active site of P450 occupied by DEN (C), residues exhibiting hydrophobic interactions with DEN are presented in the middle (B).

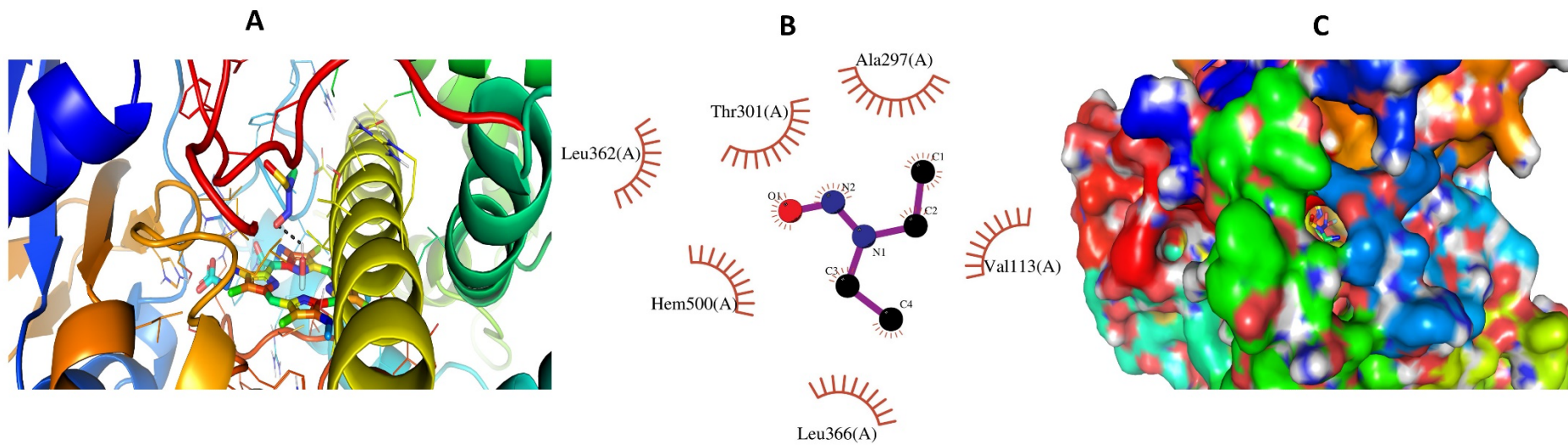


Figure 8. Binding site of DEN with P450 (CYP101D2 isozyme), DEN and P450's binding pocket are represented as tube model, while residues are shown as stick model (A), surface representation of the active site of P450 occupied by DEN (C), residues exhibiting hydrophobic interactions with DEN are presented in the middle (B).

COMPUTATIONAL Details

DFT calculations

Density-functional theoretical calculations were performed by using Gaussian 09⁴³ package for the mechanisms represented in scheme 1. Cpd I of P450's active site was represented as an oxo-ferryl species^{14, 15, 19} $\text{Fe}^{4+}\text{O}^{2-}(\text{C}_{20}\text{N}_4\text{H}_{12})^-(\text{SH})^-$. Geometry optimizations for all species in HS and LS states were performed using the UB3LYP⁴⁴⁻⁴⁷ functional in combination with the double- ζ LANL2DZ basis set for iron and 6-31G* basis set for the other atoms (BS1). Frequency calculations were also obtained at the same level of theory to depict the stationary points, to obtain zero-point energy (ZPE), to evaluate the imaginary frequency for the transition states and to confirm the ground states having no imaginary frequency. Subsequently, single-point energy calculations were performed with the LANL2DZ (F) (Fe)/6-311+G** (H,C,N,O,S) basis set (BS2) in gas phase ($\epsilon=1$) and in chlorobenzene solvent ($\epsilon=5.7$) to simulate the bulk polarity effects of the protein environment^{16, 48, 49}. For the solvation effect, the self-consistent reaction field (SCRF) method was employed using the polarizable continuum model (PCM).^{50, 51} Also, several transition states were subjected to additional intrinsic reaction coordinate (IRC) calculations to depict their paths.

Molecular dynamics simulations

To recover the final step of the process under investigation, the ADMP method of ab initio MD simulation is employed for the classical trajectory calculation at the same level of theory. The ADMP simulation was performed with simulation time of 200 femtosecond (fs) with a time interval of 0.1 fs and an initial kinetic energy about 6.3 kcal/mol. The selection of the velocities and momentums along the transition-state coordinate was done randomly. To assess the final steps of the α -mechanism, we estimated a total of 100 trajectories of each spin to figure out the development of rebound transition state (TS-reb $_{\alpha}$) in both HS and LS states. All calculations presented in MD simulations are performed using the Gaussian 09 software package.⁴³

Molecular Docking analysis

Molecular docking assessment was carried out by means of Autodock Tools (ADT) v1.5.6 and AutoDock Vina software⁵². The three-dimensional crystal structures employed for this study were obtained from the Protein Data Bank (PDB). Three cytochrome P450 isozymes were utilized for this docking analysis namely: CYP3A4 (PDB ID: 2V0M, 2.8 Å resolution), CYP2D6 (PDB ID: 2F9Q, 3 Å resolution) and CYP101D2 (PDB ID: 3NV5, 2.4 Å resolution). The crystal structure of 3NV5 was optimized for docking by adding missing residues through MODELLER 9.22 software through the direction of the 3NV6 (PDB ID) crystal structure.⁵³ Images generation polar and hydrophobic interactions detection, and output analysis were performed using PyMOL v2.3.2. The initial structure of DEN was geometrically optimized using Gaussian 09 software package⁴³ at the B3LYP level⁴⁵⁻⁴⁷ with the 6-311G (d, p) basis set.⁵⁴ DEN was docked at different active sites in the central channel of both structures of P450. UCSF Chimera was employed for initial macromolecular optimization including initial visualization and removal of ligands, solvent and all non-standard residues from the original pdb structure.⁵⁵ The adapted target protein was optimized for the docking run using ADT software, this optimization process includes adding polar hydrogens and adjusting the grid box to the most appropriate binding pocket.¹²

CONCLUSION

To sum up, we have carried out intensive computational calculations to study the proposed mechanisms for DEN-P450 interaction in water bio-catalyzed form and in uncatalyzed form. The outputs of our calculations illustrate different pathways involved in DEN-P450 catalyzed biotransformation including mainly denitrosation and dealkylation routes on α -carbon and only dealkylation pathway on β -carbon of DEN. Our findings showed that interaction of DEN with P450 at α -site is thermodynamically more favorable than β -ones as a result of the low α -H-abstraction energy barriers and the more stable secondary radical

intermediate formed in the α -pathway. In addition, the H-abstraction process in α -path is likely to proceed via two spin states: high-spin (HS, quartet) and low-spin (LS, doublet). We were able to deduce that two factors are affecting toxification and detoxification capability of DEN-P450 mechanisms including energy of denitrosation metabolites and HS rebound energy barrier of α -mechanism. Thus, existence of water as biocatalysts results in minimizing energy of denitrosation products and elevated the energy of α -HS rebound barriers. Consequently, these two influences of water biocatalysis results in enhancing the desirable detoxification pathway and thus attenuate mutagenicity and carcinogenicity of DEN. The MD simulations of the last step of the α -pathway showed that the dealkylation is fast and energetically an easy-going process at HS state. However, the inspection over the 100 of studied trajectories pointed out that the statistically most dominant process is the detachment of NO from DEN after the H-abstraction. Molecular docking analysis revealed the compatibility of DEN to P450's main active site mainly through polar bonding and hydrophobic interactions.

Conflicts of Interest:

Authors declare that there is no conflict of interest.

Acknowledgments:

This work was carried out with the financial support from PID2019-110091GB-I00 (MICINN) of the Ministerio de Ciencia, Innovación y Universidades of Spain and the PRIES-CM project Ref: Y2020/EMT-6290 from the Comunidad Autónoma de Madrid. The authors would also like to thank the Centro de Computación Científica of the UAM (CCC-UAM) for the generous allocation of computer time and for their continued technical support.

References:

- 1 F. P. Guengerich, *Nat. Rev. Drug Discovery*, 2002, **1**, 359-366.
- 2 M. A. Correia and P. R. Ortiz de Montellano, in *Cytochrome P450: Structure, Mechanism, and Biochemistry*, ed. P. R. Ortiz de Montellano, Springer US, Boston, MA2005, pp. 247-322.
- 3 D. W. Nebert and T. P. Dalton, *Nat. Rev. Cancer*, 2006, **6**, 947-960.
- 4 T. Shimada, C. L. Hayes, H. Yamazaki, S. Amin, S. S. Hecht, F. P. Guengerich and T. R. Sutter, *Cancer Res.*, 1996, **56**, 2979-2984.
- 5 F. P. Guengerich, *Chemical research in toxicology*, 2007, **21**, 70-83.
- 6 S. Shaik, S. Cohen, Y. Wang, H. Chen, D. Kumar and W. Thiel, *Chem. Rev.*, 2010, **110**, 949-1017.
- 7 T. Kamachi and K. Yoshizawa, *J. Am. Chem. Soc.*, 2003, **125**, 4652-4661.
- 8 R. Zhang, P. Li, R. Zhang, X. Shi, Y. Li, Q. Zhang and W. Wang, *J. Hazard. Mater.*, 2021, **414**, 125457.
- 9 D. Li, Y. Wang and K. Han, *Coord. Chem. Rev.*, 2012, **256**, 1137-1150.
- 10 P. O. de Montellano, *Free Radical Biology and Medicine*, 1996, **2**, 251.
- 11 P. R. Ortiz de Montellano and J. J. De Voss, in *Cytochrome P450: Structure, Mechanism, and Biochemistry*, ed. P. R. Ortiz de Montellano, Springer US, Boston, MA2005, pp. 183-245.
- 12 E. M. Kamel and A. M. Lamsabhi, *Org. Biomol. Chem.*, 2020, **18**, 3334-3345.
- 13 L. Chai, S. Ji, S. Zhang, H. Yu, M. Zhao and L. Ji, *Chem. Res. Toxicol.*, 2020, **33**, 1442-1448.
- 14 F. Ogliaro, N. Harris, S. Cohen, M. Filatov, S. P. de Visser and S. Shaik, *J. Am. Chem. Soc.*, 2000, **122**, 8977-8989.
- 15 S. P. de Visser, F. Ogliaro, P. K. Sharma and S. Shaik, *J. Am. Chem. Soc.*, 2002, **124**, 11809-11826.
- 16 L. Ji and G. Schüürmann, *J Phys. Chem. B*, 2012, **116**, 903-912.
- 17 J. P. T. Zaragoza, T. H. Yosca, M. A. Siegler, P. Moënne-Loccoz, M. T. Green and D. P. Goldberg, *J. Am. Chem. Soc.*, 2017, **139**, 13640-13643.
- 18 M. Hata, Y. Hirano, T. Hoshino and M. Tsuda, *J. Am. Chem. Soc.*, 2001, **123**, 6410-6416.
- 19 C. Li, W. Wu, K. B. Cho and S. Shaik, *Chem. Eur. J.*, 2009, **15**, 8492-8503.
- 20 Y. Wang, D. Kumar, C. Yang, K. Han and S. Shaik, *J. Phys. Chem. B*, 2007, **111**, 7700-7710.
- 21 N. Thellamurege and H. Hirao, *Molecules*, 2013, **18**, 6782-6791.
- 22 D. Wang, J. Zheng, S. Shaik and W. Thiel, *J. Phys. Chem. B*, 2008, **112**, 5126-5138.
- 23 D. Kumar, A. Altun, S. Shaik and W. Thiel, *Faraday Discuss.*, 2011, **148**, 373-383.
- 24 J. Zheng, D. Wang, W. Thiel and S. Shaik, *J. Am. Chem. Soc.*, 2006, **128**, 13204-13215.
- 25 A. Altun, V. Guallar, R. A. Friesner, S. Shaik and W. Thiel, *J. Am. Chem. Soc.*, 2006, **128**, 3924-3925.
- 26 A. Tricker and R. Preussmann, *Mutat. Res., Genet. Toxicol.*, 1991, **259**, 277-289.
- 27 L. Márquez-Rosado, M. C. Trejo-Solís, C. M. García-Cuéllar and S. Villa-Treviño, *J. Hepatol.*, 2005, **43**, 653-660.
- 28 F. P. Guengerich, *Chem. Res. Toxicol.*, 2001, **14**, 611-650.
- 29 F. P. Guengerich, C.-H. Yun and T. L. Macdonald, *J Bio. Chem.*, 1996, **271**, 27321-27329.

- 30 W. Lijinsky, *Chemistry and biology of N-nitroso compounds*, Cambridge University Press 1992.
- 31 C. Janzowski, B. Pool, R. Preussmann and G. Eisenbrand, *Carcinogenesis*, 1982, **3**, 155-159.
- 32 K. Appel, C. Rühl and A. Hildebrandt, *IARC scientific publications*, 1983, 443-451.
- 33 D. Wade, C. S. Yang, C. J. Metral, J. M. Roman, J. A. Hrabie, C. W. Riggs, T. Anjo, L. K. Keefer and B. A. Mico, *Cancer Res.*, 1987, **47**, 3373-3377.
- 34 H. Basch, K. Mogi, D. G. Musaev and K. Morokuma, *J. Am. Chem. Soc.*, 1999, **121**, 7249-7256.
- 35 J.-S. H. Yoo, F. P. Guengerich and C. S. Yang, *Cancer Res.*, 1988, **48**, 1499-1504.
- 36 A. J. Streeter, R. W. Nims, P. R. Sheffels, Y.-H. Heur, C. S. Yang, B. A. Mico, C. T. Gombar and L. K. Keefer, *Cancer Res.*, 1990, **50**, 1144-1150.
- 37 S. P. de Visser, D. Kumar, S. Cohen, R. Shacham and S. Shaik, *J. Am. Chem. Soc.*, 2004, **126**, 8362-8363.
- 38 J. F. Wang, C. C. Zhang, D. Q. Wei and Y. X. Li, *Chin. Sci. Bull.*, 2010, **55**, 1877-1880.
- 39 S.-K. Yim, K. Kim, S. Chun, T. Oh, W. Jung, K. Jung and C.-H. Yun, *J. Marine Drugs*, 2020, **18**, 603.
- 40 L. Basheer, K. Schultz and Z. Kerem, *J Scientific reports*, 2016, **6**, 1-13.
- 41 P. Banerjee, M. Dunkel, E. Kemmler and R. Preissner, *J Nucleic acids research*, 2020, **48**, W580-W585.
- 42 C. A. Hunter, J. Singh and J. M. Thornton, *J. Mol. Bio.*, 1991, **218**, 837-846.
- 43 M. J. Frisch, G. W. Trucks, H. B. Schlegel, G. E. Scuseria, M. A. Robb, J. R. Cheeseman, G. Scalmani, V. Barone, B. Mennucci, G. A. Petersson, H. Nakatsuji, M. Caricato, X. Li, H. P. Hratchian, A. F. Izmaylov, J. Bloino, G. Zheng, J. L. Sonnenberg, M. Hada, M. Ehara, K. Toyota, R. Fukuda, J. Hasegawa, M. Ishida, T. Nakajima, Y. Honda, O. Kitao, H. Nakai, T. Vreven, J. A. Montgomery Jr., J. E. Peralta, F. Ogliaro, M. J. Bearpark, J. Heyd, E. N. Brothers, K. N. Kudin, V. N. Staroverov, R. Kobayashi, J. Normand, K. Raghavachari, A. P. Rendell, J. C. Burant, S. S. Iyengar, J. Tomasi, M. Cossi, N. Rega, N. J. Millam, M. Klene, J. E. Knox, J. B. Cross, V. Bakken, C. Adamo, J. Jaramillo, R. Gomperts, R. E. Stratmann, O. Yazyev, A. J. Austin, R. Cammi, C. Pomelli, J. W. Ochterski, R. L. Martin, K. Morokuma, V. G. Zakrzewski, G. A. Voth, P. Salvador, J. J. Dannenberg, S. Dapprich, A. D. Daniels, Ö. Farkas, J. B. Foresman, J. V. Ortiz, J. Cioslowski and D. J. Fox, Gaussian 09, revision D. 01; Gaussian, Inc, in Wallingford, CT 2009.
- 44 A. D. Becke, *J. Chem. Phys.*, 1992, **96**, 2155-2160.
- 45 A. D. Becke, *J. Chem. Phys.*, 1993, **98**, 5648-5652.
- 46 A. D. Becke, *Phys. Rev. A*, 1988, **38**, 3098.
- 47 C. Lee, W. Yang and R. G. Parr, *Phys. Rev. B*, 1988, **37**, 785.
- 48 B. Honig and A. Nicholls, *Science*, 1995, **268**, 1144-1149.
- 49 C. N. Schutz and A. Warshel, *Proteins: Struct., Funct., Bioinf.*, 2001, **44**, 400-417.
- 50 S. Miertuš, E. Scrocco and J. Tomasi, *Chem. Phys.*, 1981, **55**, 117-129.
- 51 J. Tomasi, B. Mennucci and R. Cammi, *Chem. Rev.*, 2005, **105**, 2999-3094.
- 52 O. Trott and A. J. Olson, *J. Comput. Chem.*, 2010, **31**, 455-461.
- 53 A. Šali and T. L. Blundell, *J. Mol. Bio.*, 1993, **234**, 779-815.
- 54 W. J. Hehre, L. Radom, P. v. R. Schleyer and J. A. Pople, *Ab initio molecular orbital theory*, Wiley New York et al. 1986, vol. 67.

55 E. F. Pettersen, T. D. Goddard, C. C. Huang, G. S. Couch, D. M. Greenblatt, E. C. Meng and T. E. Ferrin, *J. Comput. Chem.*, 2004, **25**, 1605-1612.